Ab initio potential energy surface for the Ar (1 S)+ OH (X 2 Π) interaction and bound rovibrational states

Jacek Klos, Grzegorz Chalasinski, Mary T. Berry, Rick A. Kendall, Rudolf Burcl, M. M. Szczesniak, and Slawomir M. Cybulski

Citation: The Journal of Chemical Physics **112**, 4952 (2000); doi: 10.1063/1.481049
View online: http://dx.doi.org/10.1063/1.481049
View Table of Contents: http://scitation.aip.org/content/aip/journal/jcp/112/11?ver=pdfcov
Published by the AIP Publishing

Ab initio potential energy surface for the $Ar(^1S)+OH(X^2\Pi)$ interaction and bound rovibrational states

Jacek Klos and Grzegorz Chalasinski
Department of Chemistry, University of Warsaw, Pasteura 1, 02-093 Warszawa, Poland

Mary T. Berry
Department of Chemistry, University of South Dakota, Vermillion, South Dakota 57069

Rick A. Kendall
High Performance Computational Chemistry Group, Environmental Molecular Sciences Laboratory, Pacific Northwest National Laboratory,[a] Richland, Washington 99352-0999

Rudolf Burcl and M. M. Szczesniak
Department of Chemistry, Oakland University, Rochester, Michigan 48309

Slawomir M. Cybulski
Department of Chemistry, Miami University, Oxford, Ohio 45056

(Received 30 September 1999; accepted 23 December 1999)

Adiabatic potential energy surfaces for the $^2A'$ and $^2A''$ states of the $Ar(^1S)-OH(X^2\Pi)$ complex were calculated using supermolecular unrestricted fourth-order Møller–Plesset perturbation theory and a large correlation consistent basis set supplemented with bond functions. The potential energy surface (PES) of the A' state has two minima. The global minimum from the unrestricted coupled-cluster calculations with single, double, and noniterative triple excitations occurs for the collinear geometry Ar–H–O at $R=7.08a_0$ with a well depth of $D_e=141.2\,cm^{-1}$. There is also a local minimum for the skewed T-shaped form, whereas the Ar–O–H arrangement corresponds to a saddle point. The PES of the A'' state also has two minima, which occur for the two collinear isomers. A variational calculation of the bound rovibrational states was performed. The calculated binding energy, $D_0=93.8\,cm^{-1}$, and the energies of the bound vibrational states are in good agreement with experiment [see Berry *et al.*, Chem. Phys. Lett. **178**, 301 (1991) and Bonn *et al.*, J. Chem. Phys. **112**, 4942 (2000), preceding paper]. © *2000 American Institute of Physics.* [S0021-9606(00)01211-3]

I. INTRODUCTION

The importance of a hydroxyl radical stems from its ubiquity in atmospheric chemistry[1] and combustion processes.[2] It is involved in many hydrogen abstraction reactions which include oxidation of H_2, CH_4, and a variety of hydrocarbons. The $H_2+OH\rightarrow H_2O+H$ reaction is one of several possible models for such reactions. A simplified, but equally important, probe of the entrance channel of this process is provided by the inelastic collision process of OH and a rare-gas atom (RG). The advantage of the latter is that it can be characterized at a high level of accuracy.

Over the past decade there has been a great deal of experimental and theoretical interest in the open-shell system Ar–OH.[3–11] Its ground state, $Ar–OH(X^2\Pi)$, has been thoroughly characterized by the stimulated emission pumping (SEP) technique.[3–5] Using SEP, Lester and co-workers identified virtually all of the bound vibrational levels of $Ar–OH(X^2\Pi)$, from the zero-point level to the dissociation limit. In addition, many metastable levels have been detected as much as 200 cm^{-1} above the OH $(X^2\Pi)+Ar$ dissociation limit. These data have been used to characterize a considerable portion of the intermolecular potential energy surface (PES) at both long and short range.[5,6] The inversion of these data has led Dubernet and Hutson[6] to the first reliable semiempirical potential of Ar–OH.

In parallel with the experimental research, there has been a substantial amount of theoretical work. Degli Esposti and Werner (DEW) have performed high-quality *ab initio* calculations in the coupled electron pair approximation (CEPA), and have obtained PESs for Ar–OH in both $X^2\Pi$ and $A^2\Sigma^+$ states.[7] This PES was subsequently used to simulate the electronic and rovibrational spectra.[12(a),13,14] The DEW calculations provided the first *ab initio* mapping of the PES. In the early 1990s these results represented the state-of-the-art. However, the CEPA method, due to neglect of triple excitations, is known to underestimate the dispersion energy which is a primary binding factor in the Ar–OH complex. In addition, the basis set used by Degli Esposti and Werner is now known to be inadequate.

The aim of this work is to provide an improved *ab initio* potential energy surface for $Ar–OH(X^2\Pi)$, obtained using Møller–Plesset perturbation theory (MPPT) and an augmented correlation consistent basis set extended with bond functions. We applied the supermolecular approach based on

[a]Pacific Northwest National Laboratory is operated for the U.S. Department of Energy by Battelle Memorial Institute under contract DE-AC06-76RLO 1830.

the unrestricted Møller–Plesset perturbation theory which was accompanied by the intermolecular unrestricted Møller–Plesset perturbation theory (I-UMPPT)—a symmetry-adapted perturbation theory (SAPT) formalism applicable to open-shell systems derived recently.[15,16] I-UMPPT is a generalization of intermolecular Møller–Plesset perturbation theory (I-MPPT), a SAPT formalism designed for interactions of closed-shell systems.[17,18] Both I-MPPT and I-UMPPT are based on the Møller–Plesset zeroth-order Hamiltonian, and can provide insight into the supermolecular interaction energy. A successful application of the combination of supermolecular and intermolecular UMPPT has been recently reported by us for the He–Cl_2,[15] He–O_2,[16] Ar–O_2,[19] He–CH,[20] Ar–NH,[21] and RG–Cl[22] interactions.

The *ab initio* calculations of this work resulted in analytical fits of the Ar–OH($X^2\Pi$) PESs. The fitted functional form was used in a variational calculation of the bound rovibrational states of the complex.

II. METHOD

A. *Ab initio* calculations of the A' and A'' adiabatic potentials

The electronic configuration of the OH radical in the $X^2\Pi$ state is $1\sigma^2 2\sigma^2 3\sigma^2 1\pi^3$ and gives rise to two electronic states of the Ar–OH complex, $^2A'$ and $^2A''$.[7] These states and the associated potential energy surfaces, $V_{A'}$ and $V_{A''}$, originate from two different orientations of the Ar atom with respect to the singly occupied 1π orbital of OH: $^2A'$ corresponds to the 1π orbital with the unpaired electron located in the Ar–O–H plane, and $^2A''$ corresponds to the singly occupied 1π orbital perpendicular to the O–H–Ar plane.

The calculations of the adiabatic potentials were performed by the supermolecular approach and the interaction energy was obtained as the difference between the energies of the dimer and the monomers:

$$\Delta E^{(n)} = E_{AB}^{(n)} - E_A^{(n)} - E_B^{(n)}. \tag{1}$$

The superscript (n) denotes the level of theory, such as UHF, UMPn, UCCSD, etc. All the terms in Eq. (1) are evaluated with the same (dimer) basis set. This approach is equivalent to the counterpoise method of Boys and Bernardi.[23–25]

The ΔE^{UHF} and $\Delta E^{(2)}$ (second-order Møller–Plesset correction) terms are interpreted in the framework of the intermolecular Møller–Plesset perturbation theory (I-MPPT). This encompasses well-defined terms with a clear physical meaning, such as electrostatics, exchange, induction, and dispersion. More information about the connection between supermolecular and I-MPPT terms in the open-shell case can be found in Refs. 15 and 16.

In contrast to the interactions of closed-shell species, the counterpoise procedure for open-shell complexes causes an additional complication for any nonlinear configuration of the complex. The $C_{\infty v}$ symmetry of the OH radical in the presence of ghost orbitals of its partner is lowered to the C_s group and gives rise to two different counterpoise corrections related to the A' and A'' symmetries.[15] Another problem in applying UMPPT is the spin contamination. In all our supermolecular and perturbation calculations the spin contamination of both the OH radical as well as the Ar–OH complex was negligible, with S^2 equal to 0.752 instead of 0.750. It is important that both the dimer and monomer must have practically the same spin contamination; otherwise, the subtraction of the dimer and monomer energies is inconsistent and the interaction energies become nonsensical.

The calculations were carried out by using the GAUSSIAN 92[26] suite of programs and the new version of intermolecular perturbation theory package TRURL 94[27] which includes I-UMPPT corrections.

B. Geometries and basis sets

To describe the Ar–OH complex, it is convenient to use polar coordinates R and θ, where R denotes the distance between the center of mass of the OH radical and the Ar atom, and θ denotes the angle between the R vector and the OH bond axis. $\theta=0°$ corresponds to the Ar–H–O collinear arrangement. The O–H interatomic separation in the $^2\Pi$ state has been kept rigid at the value $r=1.95a_0=1.0319$ Å. This value is the same as the one used by Degli Esposti and Werner, but is slightly different from the equilibrium bond length given by Huber and Herzberg[28] ($r_e=0.96966$ Å, $r_0=0.9791$ Å).

The augmented correlation consistent basis set *aug-cc-pvtz*[29] has been used throughout this study. It has been augmented with a set of bond functions [3*s*3*p*2*d*] (with the exponents *sp*:0.9,0.3,0.1; *d*:0.6,0.2) hereafter denoted *aug-cc-pvtz+bf*.[18,30] Bond functions were centered in the middle of the R vector.

C. Surface fits

The UMP4/aug-cc-pvtz+bf results for $V_{A'}$, $V_{A''}$, and V_{sum} (V_{sum} defines the average of $V_{A'}$ and $V_{A''}$) were fitted to the following expression containing the short-range part, V_{sh}, and the asymptotic long-range part, V_{as}:

$$V(R,\theta) = V_{\mathrm{sh}}(R,\theta) + V_{\mathrm{as}}(R,\theta), \tag{2}$$

where

$$V_{\mathrm{sh}}(R,\theta) = G(R,\theta)\exp\left(D(\theta) - B(\theta)R\right), \tag{3}$$

$D(\theta)$ and $B(\theta)$ were expanded in Legendre polynomials $P_l^0(\cos\theta)$ up to the order $l=5$ and

$$G(R,\theta) = \sum_{l=0}^{L_2} \left(q_0^l + q_1^l R + q_2^l R^2 + q_3^l R^3\right) \times \frac{1}{\sqrt{2l+1}} P_l^0(\cos\theta) \tag{4}$$

up to the order $L_2=5$. The asymptotic part included a standard damped-dispersion expression, which was truncated at the sixth power of the inverse R (this truncation was found to be sufficiently accurate):

$$V_{\mathrm{as}}(R,\theta) = \sum_{n=6}^{n_{\max}} \sum_{\substack{l=0,2,\ldots \\ \text{or } l=1,3,\ldots}}^{n-4} f_n(B(\theta)R)\frac{C_n^{0l}}{R^n}\frac{1}{\sqrt{2l+1}} P_l^0(\cos\theta), \tag{5}$$

where f_n was the Tang–Toennies damping function:

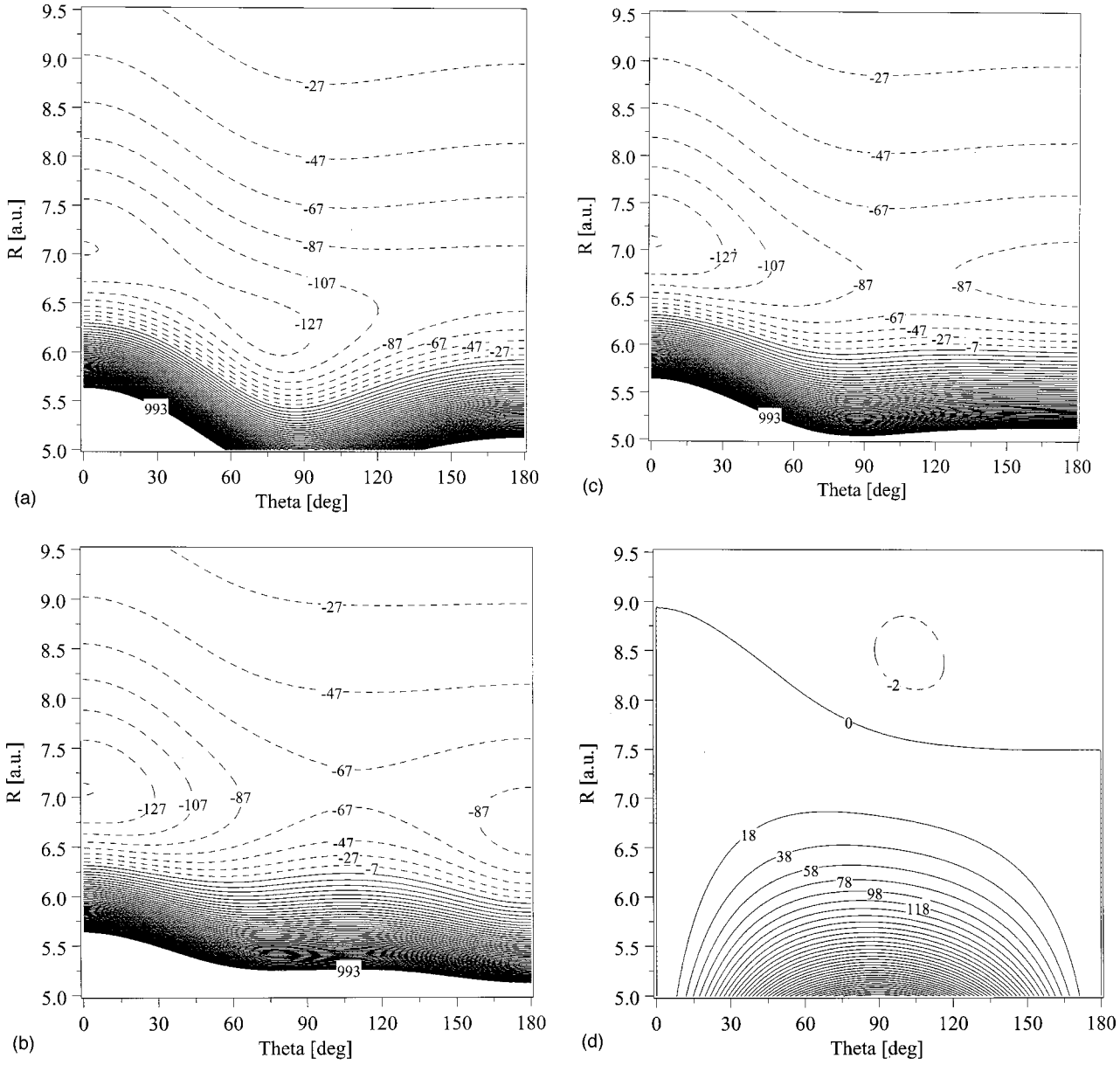

FIG. 1. (a) Contour plot of the A' state potential of the $\mathrm{Ar}(^1S)-\mathrm{OH}(X^2\Pi)$ complex ($\theta=0°$ corresponds to the Ar–HO structure). (b) Contour plot of the A'' state potential of the $\mathrm{Ar}(^1S)-\mathrm{OH}(X^2\Pi)$ complex ($\theta=0°$ corresponds to the Ar–HO structure). (c) Contour plot of the V_{sum} potential ($\theta=0°$ corresponds to the Ar–HO structure). (d) Contour plot of the V_{diff} potential ($\theta=0°$ corresponds to the Ar–HO structure).

$$f_n(x)=1-e^{-x}\sum_{k=0}^{n}\frac{x^k}{k!}. \tag{6}$$

Only the assymptotic term of Eq. (5) with $n=6$ and $l=0$ was used in the fit. The functional form adopted for the V_{diff} (defined as a half of the difference of $V_{A''}$ and $V_{A'}$) differed from the above by replacing $P_l^0(\cos\theta)$ in $G(R,\theta)$ and in V_{as} [but not in the damping factor Eq. (6)] by $P_l^2(\cos\theta)$, and by dropping the $1/\sqrt{2l+1}$ term. The limiting values of summations were as follows: $l=1$, $L_2=7$, $n_{\max}=9$, and $l=2-5$. The rms errors of the analytical representations of the V_{sum} and V_{diff} are 3.5 and 0.7 cm^{-1}, respectively. For the purpose of rovibrational calculations the V_{sum} and V_{diff} potentials have also been cast into the form of Degli Esposti and Werner,[7] for each angle θ_k:

$$b_l(R)=e^{-a_l(R-R_l)}\left(\sum_{i=0}^{3}b_l^{(i)}R^i\right)-\frac{1}{2}\left[1+\tanh\left(\frac{(R-S_l)}{T_l}\right)\right]\sum_{j=3}^{4}C_l^{(2j)}R^{-2j}. \tag{7}$$

The error of refitting did not exceed 0.25 cm^{-1} for V_{sum} and 0.12 cm^{-1} for V_{diff}. Contour plots of the A' and A'' PESs are shown in Fig. 1. The values of the parameters for $V_{A'}$, $V_{A''}$, V_{sum}, and V_{diff} as well as the FORTRAN code generating these quantities are available on request.[31]

TABLE I. Interaction energies for OH($X^2\Pi$)+Ar(^1S) at different levels of the supermolecular approach close to different stationary forms: collinear and T-shaped (energies in μE_h). The results have been obtained with the aug−cc−pvtz+bf, the value in parenthesis refer to aug−cc−pvtz.

	Ar–H–O $R=7a_0$	Ar–O–H $R=6.9a_0$	T-shaped $6.5a_0$, 120° A'	T-shaped $6.5a_0$, 120° A''
ΔE^{UHF}	414.10	185.70	394.56	760.87
$\Delta E(2)$	−629.80	−404.00	−540.94	−172.14
$\Delta E(3)$	−537.90	−353.60	−476.00	−143.36
$\Delta E(4)$	−671.00	−423.6	−598.82	−255.39
$\Delta E^{\mathrm{CCSD(T)}}$	−643.50	−414.8	−596.49	−250.48
	(−559.9)	(−348.8)		

III. RESULTS AND DISCUSSION

A. Features of total PES

The interaction energies were obtained at the UMP4/aug-cc-pvtz+bf level of theory, for a wide range of intermolecular distances, from $5.0a_0$ to $10.0a_0$, and for angles from 0° to 180°. The PESs for the A' and A'' states are shown in Figs. 1(a) and 1(b) (see also Ref. 32).

The PES of the A' state has two minima. The global minimum occurs for the collinear geometry Ar–H–O ($R=7.08a_0$, $\theta=0°$ and $D_e=147.3\,\mathrm{cm}^{-1}$). The UCCSD(T) estimate of D_e is only slightly smaller and amounts to 141.2 cm^{-1}. There is also a local minimum for the skewed T-shaped geometry ($R_e=6.23a_0$, $\theta_e=75.1°$) with $D_e=135.5\,\mathrm{cm}^{-1}$. The Ar–O–H geometry corresponds to a saddle point at $6.70a_0$ elevated 51.8 cm^{-1} above the global minimum.

The PES for the A'' state has two minima for the two collinear forms: Ar–O–H and Ar–H–O. As with the A' state, the global minimum occurs for the Ar–H–O configuration, and has the same parameters. The local minimum for the Ar–O–H configuration is characterized by $R_e=6.70a_0$, and $D_e=95.5\,\mathrm{cm}^{-1}$.

The two surfaces have qualitatively different anisotropies. In order to explain these differences the total interaction energies were dissected into the I-UMPPT components. The analysis of the interaction energy components revealed that the major factor which distinguishes the A' and A'' states is the exchange energy. Whereas the global, ''hydrogen-bonded,'' Ar–H–O minimum is determined by the dispersion attraction enhanced by the induction effects, the local minima are due to the locally reduced exchange repulsion. This is the origin of the T-shaped minimum for A' and the Ar–O–H minimum for A''.

B. Convergence of S-UMPPT and basis set unsaturation effects

The convergence of UMPPT through the fourth order is shown in Table I. Interestingly, it is very similar for both the A' and A'' states. The major repulsive contribution is included in the UHF interaction energy while the major attractive contribution is encompassed in the second order $\Delta E^{(2)}$. The $\Delta E^{(3)}$ and $\Delta E^{(4)}$ corrections are smaller, but important from a quantitative point of view. The pattern of convergence does not qualitatively depend on the mutual Ar-radical orientation, and it is typical for the Ar-molecule complexes: (i) $\Delta E^{(3)}$ is repulsive and deteriorates the MP2 approximation, and (ii) $\Delta E^{(4)}$ is attractive and somewhat larger in magnitude than $\Delta E^{(3)}$. Finally, the UCCSD(T) level of theory reduces the UMP4 interaction only by a few percent. To summarize, the convergence through the fourth order as well as the UCCSD(T) results are typical for closed-shell molecule interaction with Ar, and thus UMP4 is expected to be sufficient to provide highly accurate results (about ±5%).

Saturation of the basis set is another problem. The aug-cc-pvtz when used with bond functions is known capable of providing highly accurate results.[18,30,33] Our experience is that for a closed-shell system the PES near the minimum should be accurate to within ±5%. We expect a similar accuracy in the Ar–OH case as well.

Our best estimate of $D_e=141.2\,\mathrm{cm}^{-1}$ is compatible with the calculations of Degli Esposti and Werner.[7] The latter authors obtained $D_e=102\,\mathrm{cm}^{-1}$ by means of the CEPA method with an extended basis set through the f orbitals. In view of the evidence reported by Chalasinski and Szczesniak,[18] such a strategy is likely to provide interaction energies about 30% too small.

Our value of $D_e=141.2\,\mathrm{cm}^{-1}$ is also considerably larger than the semiempirical estimate of 126 cm^{-1} obtained by Dubernet and Hutson.[6] We expect that future empirical evaluation of D_e will bring this value significantly closer to our result.

C. Calculations of Ar–OH($X^2\Pi$) bound states

1. Method

A variational calculation of the bound rovibrational states supported by the potential was performed as described in Ref. 12(a), except that a sign error in Eq. (18) of that work was corrected as in Eq. (9) of Ref. 12(b). Briefly, an optimal radial basis set, $\{|v_s\rangle\}$, was found by diagonalizing the matrix of a stretching Hamiltonian, using an initial basis set of distributed Gaussian functions. The stretching Hamiltonian was defined by

$$\mathrm{H_{str}}=-\frac{\hbar^2}{2\mu R}\frac{\partial^2}{\partial R^2}R+V_{\mathrm{str}}(R), \tag{8}$$

where $V_{\mathrm{str}}(R)$ is the isotropic component in the expansion of V_{sum} in terms of Legendre polynomials. The optimal angular basis set, $\{|v_b\rangle\}$ was derived using an angular Hamiltonian defined as the expectation value for $|v_s=0\rangle$ of those terms in the total rovibrational Hamiltonian not included in $\mathrm{H_{str}}$:

$$\mathrm{H_{ang}}=\langle v_s=0|\mathrm{H}-\mathrm{H_{str}}|v_s=0\rangle, \tag{9}$$

where H includes the full potential energy function.

A preliminary angular basis set, which was used to construct the ''optimal'' angular basis, was formed by coupling OH rotational wavefunctions $|j(\mathrm{OH}),m,F_i,\varepsilon,{}^2\Pi\rangle$ with functions $|LM_L\rangle$, describing the angular motion of the intermolecular axis, R, with respect to the space-fixed frame, to yield functions of total angular momentum, **J**. The symmetry index of the wavefunction, $\varepsilon=\pm1$, labels states of opposite parity. $F_i, i=1,2$, labels the Hund's case (b) wavefunctions

TABLE II. Comparison between calculated and measured energies (cm^{-1}) for the bound states of $OH(^2\Pi)+Ar$. Energies are for $J=\frac{3}{2}$, except for $|v_s=0\rangle|v_b=4\rangle$ where the energy is for the lowest rotational level, $J=\frac{5}{2}$. For the UMP4 potential and for the semiempirical potential of Ref. 6, the reported energies represent the average of the two parity components. For the CEPA potential and the semiempirical potential of Ref. 5 the energies are for the positive parity component.

Assignment		Experimental	*ab initio*		Semiempirical	
v_s	v_b	Refs. 3 and 4	UMP4	CEPA [Ref. 12(a)]	Ref. 5	Ref. 6
0	0	0	0	0	0	0
	1	9.19[a]	10.8	9.2	9.5	9.7
	2	19.2	20.4	16.6	19.3	19.2
	3	21.3	21.1	17.2	21.3	21.3
1	0	34.9	34.0	27.9	34.7	34.9
	1	41	40.7	33.9	42.1	41.3
	2	50	48.1	39.1	48.9	47.8
	3	50	49.3	39.6	50.6	49.3
2	0	60	59.2	47.2	60.2	60.6
	1	64	63.7	51.0	65.9	64.6
	2	71	68.8	54.1	70.1	69.1
	3	71	70.0	54.5	71.4	70.0
3	0	78	76.6	58.7	77.3	78.1
	1	81	79.7	61.1	81.2	80.6
	2	85	82.7	62.2	83.3	83.4
	3	85	83.6	62.6	84.2	84.0
4	0		87.2			88.6
	1		89.1			90.1
	2		90.4			91.7
	3		90.9			92.0
0	4	(89)[b]	90.2	nb[c]	87.5	88.1
Binding energy						
	D_o	93–103	93.8	65.6	93.2	95.5
	D_e	⋯	147	103	127	126

[a]New measurement of $J=\frac{3}{2}$ position, see Ref. 34. This supersedes the earlier value of 9.7 cm^{-1} reported in Refs. 3 and 4.

[b]The feature in the SEP spectrum at 89 cm^{-1} was originally assigned to a transition terminating on $|v_s=0\rangle|v_b=4\rangle$ $[j(OH)=\frac{5}{2},P=\frac{5}{2}]$. Dubernet and Hutson (Ref. 6) have suggested that a SEP transition to this state is not favored by selection rules for ΔP and that the SEP feature might better be assigned to one of the $|v_s=4\rangle$ states.

[c]States correlating with $j(OH)=\frac{5}{2}$ are not predicted to be bound by the CEPA potential.

which are admixtures of states with the same $j(OH)$, m, and ε, but different $\omega=|\lambda+\sigma|$. (By convention, small letters are used to refer to quantum numbers of the diatom.) In the case (a) limit, where ω is a good quantum number, F_1 designates the lower spin-orbit component, $^2\Pi_{3/2}$, and F_2 designates the upper spin-orbit component, $^2\Pi_{1/2}$.

Diagonalizing H_{ang} in this basis yielded the optimal angular basis set $\{|v_b\rangle\}$. For a weakly anisotropic potential, $j(OH)$ is approximately conserved in the diagonalization. However, the different orientations of the diatom's total angular momentum with respect to the intermolecular axis, R, result in states with different energies, lifting the $2j(OH)+1$ degeneracy of the OH rotational level. Thus the first four levels in the optimal angular basis, $v_b=0-3$, correlate with $j(OH)=\frac{3}{2}$ and the next six, $v_b=4-9$, correlate with $j(OH)=\frac{5}{2}$. The quantum number for the projection of $\mathbf{j}(OH)$ on R is designated P. The sign convention for P is discussed in Ref. 6.

The optimal basis of product functions $\{|v_s\rangle|v_b\rangle\}$ was then used in the variational calculation for the total rovibrational Hamiltonian. The size of this product basis was restricted by a parameter, N_x, such that the sum of the indices for the stretching basis functions and the angular basis functions was less than or equal to N_x, i.e., $v_s+v_b+2\leqslant N_x$, where the addition of 2 appears because the lowest stretching and angular wavefunctions, which have indices of 1, are $v_s=0$ and $v_b=0$. Thus the size of the product basis was controlled in three ways: by the number of functions in the stretching basis, by the number of functions in the angular basis, and by the parameter N_x.

2. Rovibrational bound states

Table II gives the eigenvalues resulting from the variational calculation using the UMP4 potential along with the energies determined experimentally by SEP[3,4] and IR.[34] Also given are the energies calculated from the DEW CEPA potential[7,12a] and for two semiempirical potential energy surfaces[5,6] which were fit to the SEP data. The calculated eigenfunctions consist of a series of van der Waals stretching

modes, each of which is associated with a ''bending'' manifold. With the exception of the last level listed in Table II, all of the bound levels correlate with the lowest rotational level of OH, $j(\mathrm{OH})=\frac{3}{2}$, and the four members of the bending manifold correspond to the four different projections, P, of $\mathbf{j}$(OH) on the internuclear axis, R. The lowest two levels of each manifold have maxima in the angular probability distribution at O–H–Ar angles, $\theta \leqslant 90°$, whereas the higher two have maxima at $\theta \geqslant 90°$.

The eigenfunction for the last level listed in Table II has as its major component the basis function $|v_s=0\rangle|v_b=4\rangle$ where the bending function is derived from $j(\mathrm{OH})=\frac{5}{2}$. The energy given is for the lowest rotational level of the complex, $J=\frac{5}{2}$.

The UMP4 potential reproduces the experimental energies to within the experimental accuracy in most cases. The van der Waals stretching energies, which were underestimated by the CEPA potential, are correctly (within 3% of the experimental values) predicted by the UMP4 potential. The experimental SEP data refer to peak center positions of bands with unresolved rotational structure. For levels with $v_b=0$, this corresponds rather nearly to the rotational origin. For vibrational levels with $v_b=1-3$, the significant parity splitting of the rotational levels leads to predicted band structures for which the origin is shifted alternately to lower energy of the band center for $v_b=1$, then to higher energy for $v_b=2$ and for $v_b=3$. This has been confirmed experimentally by Bonn *et al.*[34] for $|v_s=0\rangle|v_b=1\rangle$. The SEP peak intensity lies at 9.7 cm^{-1}.[3,4] The origin lies 0.5 cm^{-1} lower at 9.2 cm^{-1}. This effect should be greatest for the $v_b=1$ levels, which exhibit the greatest parity splitting, as shown in Table III. The calculated energy levels for the UMP4 potential are the average of the positive and negative parity components of $J=\frac{3}{2}$ relative to the $J=\frac{3}{2}$ level of the ground vibrational state. This differs from the origin position (relative to the origin of the ground vibrational state) by only $3.75*\Delta B$ and, thus, only in the second decimal place. The most notable difference between experimental and calculated energies occurs at the first excited bend, which is predicted to fall 1.6 cm^{-1} higher in energy than is found experimentally, suggesting that the UMP4 potential anisotropy is too great between 0° and 90° for the range of R sampled by $|v_s=0\rangle$.

The parity splitting of the $J=\frac{3}{2}$ level of $|v_s=0\rangle|v_b=1\rangle$ state is predicted to be 0.67 cm^{-1} by the UMP4 potential. The CEPA potential predicted a splitting of 0.58 cm^{-1}.[6] The semiemperical potential of Dubernet and Hutson[6] reproduced the reported experimental value of 0.23 cm^{-1} to which it was fit. However, Dubernet and Hutson found it difficult to reconcile this small splitting with the reported magnitude of the parity splitting in the ground vibrational state.[11] Recent experiments by Bonn *et al.*[34] show that the earlier experimental value was in error, and that the correct splitting for this level is 0.69 cm^{-1}, in good agreement with the predicted splitting.

The rotor constants for the lowest two vibrational levels, $|v_s=0\rangle|v_b=0,1\rangle$ are predicted by the UMP4 potential to be 0.102 and 0.110 cm^{-1}, respectively. These may be compared to the experimental values of 0.1024 cm^{-1} for $|v_b=0\rangle$ (reported by Schleipen[35] and Oshima[11]) and 0.1115 cm^{-1} for $|v_b=1\rangle$ (Bonn *et al.*[34]). Rotor constants for the other levels are reported in Table III, but at this time there are no experimental values with which to compare them. The calculated eigenvalues given for the UMP4 potential in Table II are converged to 0.1 cm^{-1} or better. In the final variational calculation using the product basis, the angular basis set was limited to 30 functions and the radial basis to 90. The parameter N_x was set at 91 in order to further restrict the product basis. To check convergence with respect to the angular basis, the variational calculation was performed with a radial basis size of 75 ($N_x=76$) and angular bases of 20, 30, 42, and 50 functions. The eigenvalues for the $J=\frac{3}{2}(+)$ rotational states of the vibrational levels reported in Table II changed by 0.2 cm^{-1} or less when the angular basis was increased from 20 to 30. They changed by less than 0.02 cm^{-1} when the angular basis was increased to 42, and by an additional 0.001 cm^{-1} or less when the angular basis size was increased to 50. Thus, an angular basis set of 30 functions was deemed adequate to achieve an ultimate convergence of 0.1 cm^{-1}. To check convergence with respect to the radial basis, the angular basis size was fixed at 30 functions and radial bases of 45, 55, 65, 75, 85, and 90 were tested. In each case N_x was fixed at one greater than the radial basis size. Again the calculation was for the positive parity component of the $J=\frac{3}{2}$ rotational state. The levels converged at very different rates. The ground vibrational state $|v_s=0\rangle|v_b=0\rangle$ was converged to 0.01 cm^{-1} with a radial basis of 45 functions. The first bend, $|v_s=0\rangle|v_b=1\rangle$, was converged to 0.1 cm^{-1} at this point, but the eigenvalue for $|v_s=2\rangle|v_b=2\rangle$, for example, was still 0.5 cm^{-1} higher than the finally converged value. With a radial

TABLE III. Rotor constants and parity splittings for the bound vibrational states of OH–Ar for $J=\frac{3}{2}$. The rotor constants are all calculated from the expectation value $\langle 1/R^2\rangle$.

v_s	v_b	Rotor constant (cm^{-1})	Parity splitting for $J=\frac{3}{2}$ (cm^{-1})
0	0	0.102	0.00
	1	0.110	0.67
	2	0.108	−0.31
	3	0.107	−0.11
1	0	0.095	0.00
	1	0.101	0.58
	2	0.098	−0.51
	3	0.096	−0.02
2	0	0.087	0.00
	1	0.089	0.47
	2	0.086	−0.39
	3	0.083	−0.01
3	0	0.075	0.00
	1	0.074	0.36
	2	0.070	−0.25
	3	0.066	0.00
4	0	0.060	0.00
	1	0.056	0.25
	2	0.052	−0.02
	3	0.047	0.00
0	4	0.109[a]	0.00[a]

[a]For $J=\frac{5}{2}$.

basis size of 85 functions all of the eigenvalues were converged to 0.1 cm^{-1} or better.

IV. SUMMARY AND CONCLUSIONS

In our previous papers[15,16,19–21] we showed that complexes of open-shell species interacting with closed-shell rare gas atoms can, essentially, be of three different types, involving contact with either double-, single-, or unoccupied orbitals.

In the particular case of Ar–OH we have the first two possibilities: (i) when the doubly occupied orbital of an open-shell species overlaps with an orbital of the closed-shell moiety, and the singly occupied one is perpendicular to the collision plane. Such a situation is similar to a regular van der Waals interaction which occurs between closed-shell species. The second possibility is (ii) when the singly occupied orbital overlaps with an orbital of the closed-shell moiety. Then, in contrast to the closed-shell–closed-shell case, exchange repulsion is largely reduced, and van der Waals bonding becomes stronger. In certain circumstances, as, e.g., in the H_2+OH collision, this contact may open a reactive channel, which precedes the hydrogen abstraction reaction.[36]

The UMP4 surface discussed in this work represents a considerable improvement over the earlier CEPA *ab initio* surface as evidenced by the better agreement between calculated and experimentally determined energies of the bound intermolecular vibrational states.

ACKNOWLEDGMENTS

This work was performed in part under the auspices of the U.S. Department of Energy, under Contract No. DE-AC6-76RLO 1830, with Battelle Memorial Institute, which operates the Pacific Northwest National Laboratory. Some of the computational resources were provided by the Division of Chemical Sciences, Office of Basic Energy Sciences, and Office of Energy Research of the U.S. Department of Energy, and are gratefully acknowledged. These resources are operated by the National Energy Research Scientific Computing (NERSC) facility at Lawrence Berkeley National Laboratory. Partial support by the NSF (Grant No. CHE-9527099), by the Polish Committee for Scientific Research KBN (Grant 3 T09A 112 18), and by the Michigan Space Grant Consortium is also gratefully acknowledged. S. M. C. acknowledges the support of the NSF (Grant No. CHE-9616683). The authors thank D. C. Clary and C. Chakravarty who provided the code with which the variational calculation was performed. The authors also thank Marsha Lester and Millard Alexander for helpful discussions.

[1] R. P. Wayne, *Chemistry of Athmospheres: An Introduction to the Chemistry of the Atmospheres of Earth, the Planets, and their Satellites* (Oxford University Press, Oxford, 1991).
[2] J. Warnatz, U. Maas, and R. W. Dibble, *Combustion: Physical and Chemical Fundamentals, Modelling, and Simulations, Experiments, Pollutant Formation* (Springer Verlag, Berlin, 1996).
[3] M. T. Berry, M. R. Brustein, M. I. Lester, C. Chakravarty, and D. C. Clary, Chem. Phys. Lett. **178**, 301 (1991).
[4] M. T. Berry, R. A. Loomis, L. C. Giancarlo, and M. I. Lester, J. Chem. Phys. **96**, 7890 (1992).
[5] M. I. Lester, W. H. Green, Jr., C. Chakravarty, and D. C. Clary, in *Molecular Dynamics and Spectroscopy by Stimulated Emission Pumping*, edited by H. L. Dai and R. W. Field (World Scientific, Singapore, 1995), pp. 659–688.
[6] M.-L. Dubernet and J.-M. Hutson, J. Chem. Phys. **99**, 7477 (1993).
[7] A. Degli Esposti and H.-J. Werner, J. Chem. Phys. **93**, 3351 (1990).
[8] A. Degli Esposti, A. Berning, and H.-J. Werner, J. Chem. Phys. **103**, 2067 (1995).
[9] W. M. Fawzy and M. C. Heaven, J. Chem. Phys. **92**, 909 (1990).
[10] B.-C. Chang, L. Yu, D. Cullin, B. Refuss, J. Williamson, T. A. Miller, W. M. Fawzy, X. Zheng, S. Fei, and M. C. Heaven, J. Chem. Phys. **95**, 7086 (1991).
[11] Y. Oshima, M. Iida, and Y. Endo, J. Chem. Phys. **95**, 7001 (1991).
[12] (a) C. Chakravarty and D. C. Clary, J. Chem. Phys. **94**, 4149 (1991); (b) P. J. Dagdigian, M. H. Alexander, and K. Liu, *ibid.* **91**, 839 (1989).
[13] C. Chakravarty, D. C. Clary, A. D. Esposti, and H. J. Werner, J. Chem. Phys. **93**, 3367 (1990).
[14] C. Chakravarty and D. C. Clary, Chem. Phys. Lett. **173**, 541 (1990).
[15] S. M. Cybulski, R. Burcl, G. Chalasinski, and M. M. Szczesniak, J. Chem. Phys. **103**, 10116 (1995).
[16] S. M. Cybulski, R. Burcl, G. Chalasinski, and M. M. Szczesniak, J. Chem. Phys. **104**, 7997 (1996).
[17] B. Jeziorski, R. Moszynski, and K. Szalewicz, Chem. Rev. **94**, 1887 (1994).
[18] G. Chalasinski and M. M. Szczesniak, Chem. Rev. **94**, 1723 (1994).
[19] S. M. Cybulski, R. A. Kendall, G. Chalasinski, M. W. Severson, and M. M. Szczesniak, J. Chem. Phys. **106**, 7731 (1997).
[20] S. M. Cybulski, G. Chalasinski, and M. M. Szczesniak, J. Chem. Phys. **105**, 9525 (1996).
[21] R. A. Kendall, G. Chalasinski, J. Klos, R. Bukowski, M. W. Severson, M. M. Szczesniak, and S. M. Cybulski, J. Chem. Phys. **108**, 3235 (1998).
[22] R. Burcl, R. V. Krems, A. A. Buchachenko, M. M. Szczesniak, G. Chalasinski, and S. M. Cybulski, J. Chem. Phys. **109**, 2144 (1998).
[23] S. F. Boys and F. Bernardi, Mol. Phys. **19**, 553 (1970).
[24] J. H. van Lenthe, J. G. C. M. van Duijneveldt-van de Rijdt, and F. B. van Duijneveldt, Adv. Chem. Phys. **69**, 521 (1987).
[25] M. Gutowski, M. M. Szczesniak, and G. Chalasinski, Chem. Phys. Lett. **241**, 140 (1995).
[26] M. J. Frisch, G. W. Trucks, M. Head-Gordon, P. M. W. Gill, M. W. Wong, J. B. Foresman, B. G. Johnson, H. B. Schlegel, M. A. Robb, E. S. Replogle, R. Gomperts, J. L. Andres, K. Raghavachari, J. S. Binkley, C. Gonzalez, R. L. Martin, D. J. Fox, D. J. Defrees, J. Baker, J. J. P. Stewart, and J. A. Pople, GAUSSIAN 92, Gaussian, Inc., Pittsburgh, PA, 1992.
[27] S. M. Cybulski, TRURL 94 package, Rochester, MI, 1994.
[28] K. P. Huber and G. Herzberg, *Molecular Spectra and Molecular Structure, IV. Constants of Diatomic Molecules* (Van Nostrand Reinhold, New York, 1979).
[29] R. A. Kendall, T. H. Dunning, Jr., and R. J. Harrison, J. Chem. Phys. **96**, 6796 (1992); T. H. Dunning, Jr., *ibid.* **90**, 1007 (1989).
[30] R. Burcl, G. Chalasinski, R. Bukowski, and M. M. Szczesniak, J. Chem. Phys. **103**, 1498 (1995).
[31] The fit to the PES is available upon request from jakl@chem.uw.edu.pl
[32] See EPAPS Document No. EJCPSA6-112-012011 for a table of calculated A' and A'' energies. This document may be retrieved via the EPAPS homepage (http://www.aip.org/pubservs/epaps.html) or from ftp.aip.org in the directory /epaps/. See the EPAPS homepage for more information.
[33] K. W. Chan, T. D. Power, J. Jai-nhuknan, and S. Cybulski, J. Chem. Phys. **110**, 860 (1999).
[34] R. T. Bonn, M. D. Wheeler, and M. Lester, J. Chem. Phys. **112**, 4942 (2000), preceding paper.
[35] J. Schleipen, L. Nemes, J. Heinze, and J. J. ter Meulen, Chem. Phys. Lett. **175**, 561 (1990).
[36] R. L. Schwartz, D. T. Anderson, M. W. Todd, and M. I. Lester, Chem. Phys. Lett. **273**, 18 (1997); D. T. Anderson, R. L. Schwartz, M. W. Todd, and M. I. Lester, J. Chem. Phys. **109**, 3461 (1998).